HIGHLY EXCITED NUCLEAR SYSTEMS

EMISSION OF INTERMEDIATE MASS FRAGMENTS DURING FISSION

S.L. Chen, R.T. de Souza, E. Cornell, B. Davin, T.M. Hamilton, D. Hulbert,[‡]
K. Kwiatkowski, Y. Lou, and V.E. Viola
Department of Chemistry and Indiana University Cyclotron Facility, Indiana University, Bloomington, Indiana 47405

R.G. Korteling
Department of Chemistry, Simon Fraser University, Burnaby, British Columbia, Canada

J.L. Wile[†]
Department of Chemistry, Ball State University, Muncie, Indiana 47302

In a recent experiment,[1] low energy intermediate-mass fragments (IMF: $3 \leq Z \leq 6$) were observed in coincidence with fission for the reaction $^{3}He + ^{232}Th$ at E_{lab}=270 MeV. The low energy IMFs in that reaction exhibit an angular distribution peaked essentially orthogonal to the scission axis, indicative of strong focusing by the Coulomb field of the scissioning system (see Fig. 1). In contrast, the high energy fragments have no strong preference relative to the scission axis. The strong resemblance of the measured IMF energy and angular distributions to the distributions measured for neck emission of α particles during scission[2-6] suggests a common origin for both the IMFs and neck-emitted α particles.[1]

In order to understand this novel decay mode better, we have investigated emission of intermediate-mass fragments (IMF:$3 \leq Z \leq 8$) in the reaction $^{4}He + ^{232}Th$ at E_{lab}=200 MeV. The experiment was performed at IUCF where beams of ^{4}He nuclei impinged on a self-supporting $\approx$700 $\mu g/cm^2$ ^{232}Th foil. The beam intensity was typically $\approx$20 mA. Fission fragments were detected in two hybrid large-area parallel-plate avalanche multi-wire proportional (PPAC/MWPC) detectors. The centers of these detectors were located at θ_{lab}=+100.3° and −60.0° to account for the reaction kinematics. IMFs were detected in four large and five small low-threshold detector telescopes located essentially 90° to the scission axis. Two additional large telescopes were located at an angle $\approx$50° to the scission axis.

Charged particles that entered the silicon detector were identified by the ΔE-E technique. In addition, charged particles were also mass-identified by utilizing the time-of-flight technique with reference to the cyclotron RF pulse. The timing resolution achieved in the experiment was sufficient to resolve isotopes of elements with $Z \leq 4$. Energy calibration of the detectors was performed by use of a ^{228}Th α-source and a precision pulser.

The energy spectra of ternary fragments with $3 \leq Z \leq 8$ are shown in Fig. 2. Since all the spectra for detectors orthogonal to the scission axis are the same, these spectra have been summed and are represented by the closed symbols. The energy spectra for

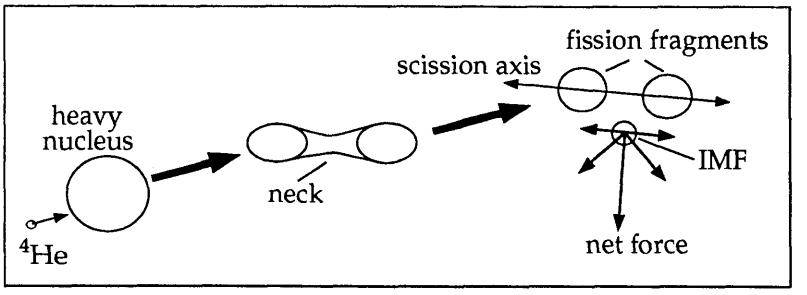

Figure 1. Top panel: Cartoon illustrating the cancellation of forces for charged particle emission from the neck zone during fission.

the non-orthogonal detectors are represented by the open symbols. These two groups of energy spectra are significantly different. For beryllium fragments, for example, the energy spectra for the orthogonal detectors is bimodal (closed symbols) and manifests a low energy component peaked at 15-20 MeV. This low-energy component is absent in the energy spectrum of the non-orthogonal detector (open symbols). Moreover, the high-energy component centered at 35-45 MeV is observed in both spectra. It is important to note that the absolute differential yield of the high-energy component is the same for both the orthogonal and non-orthogonal detectors. No re-normalization has been performed for the two sets of spectra shown in Fig. 2. While the high-energy component exhibits an "isotropic" angular distribution with respect to the scission axis, the low-energy component exists only for those detectors located near the normal to the scission axis.

These qualitative observations can be understood as follows: the high energy IMFs originate from the excited composite nuclear system in its more compact shape and hence, are subject to a larger Coulomb energy and lack angular focusing. The high energy peak occurs at the energy usually associated with IMF emission from a heavy nucleus.[7] The arrows shown in the figure indicate the calculated Coulomb barrier for emission of Li, Be, B, C, N, and O fragments, respectively, from a composite system of Z=90, A=232. The semi-quantitative agreement indicates that the high-energy IMFs are emitted from the composite system prior to significant deformation. In contrast, the low-energy fragments, which arise from neck emission near the time of scission, experience a lower Coulomb field (Fig. 1).

A striking qualitative feature of Fig. 2 is the significant enhancement in the beryllium and carbon yield over the boron yield. A similar enhancement (24%) of Be fragments over Li fragments was observed in spontaneous fission of ^{252}Cf.[8] This enhancement of even-Z nuclei over odd-Z nuclei may provide information about the excitation of the system at the time of neck IMF emission.

The trends observed in Fig. 2 are quantitatively examined in Fig. 3. Shown in panel a) are the cross-sections for both low energy/focussed (solid symbols) and high energy/isotropic (open symbols) emission of fragments with $2 \leq Z \leq 8$. The cross section was calculated from the number of interactions, the integrated beam current and the target thickness, and agreed with the previously measured binary-fission cross section to within 5%. The efficiency for detecting ternary events was calculated using the measured IMF

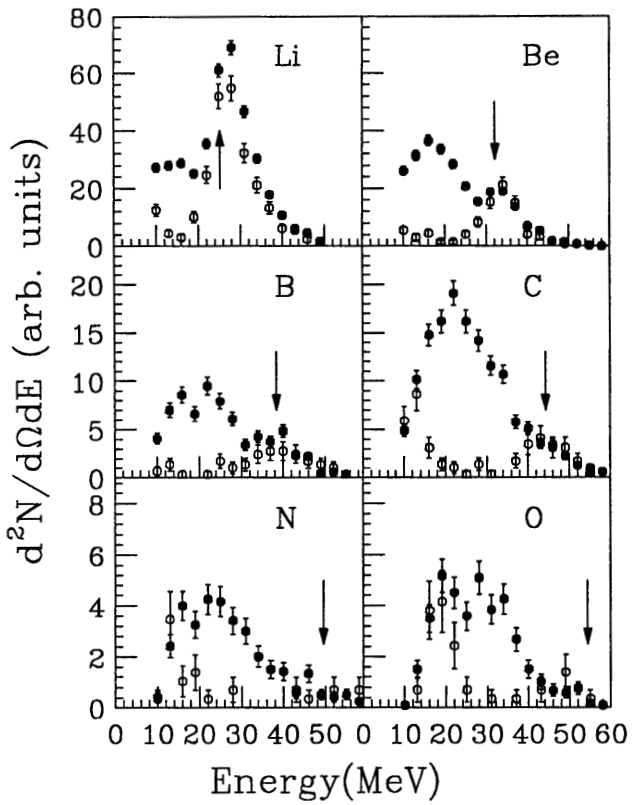

Figure 2. Laboratory energy spectra of Li, Be, B, C, N and O fragments emitted orthogonal to the fission axis (solid symbols) and approximately 50° with respect to the fission axis (open symbols).

energy distribution. The angular distribution of neck fragments was assumed to be a gaussian with a width of 15°. We estimate the uncertainty in cross section to be less than 10%. While the Z distribution for both low-energy and high-energy fragments follows the general trend of decreasing yield with increasing Z, the decrease in yield with increasing Z is less for the low-energy fragments than it is for the high-energy isotropic fragments. This same observation has been noted in the ^{3}He-induced reaction on ^{232}Th.[9] Emission of heavy IMFs is strongly favored by the neck mechanism. In addition, both the neck component and the isotropic component manifest preferential emission of even-Z nuclei. This preferential emission of even-Z nuclei is stronger for the neck component than for the isotropic component.

The dependence of the average energy on Z is shown in the second panel of Fig. 3. Essentially a linear dependence of the average energy on Z is observed. The open symbols shown in Fig. 3b) correspond to the measured $\langle E \rangle$ transformed into the center-of-mass frame (v_{cm}=0.1 cm/ns) consistent with the measured linear momentum transfer. The open diamonds in this figure correspond to the measured $\langle E \rangle$ for ^{4}He, Li, and Be in spontaneous fission of ^{252}Cf.[8]

The dependence of the second moment ($\langle\langle (E - \langle E \rangle)^2 \rangle^{1/2}$) of the low energy spectra on Z is shown as the solid points in Fig. 3c). As evident in the figure, the width of the energy spectrum for the neck component is essentially constant with atomic number for $Z \geq 4$. Since differences in the scission configuration and in the thermal distribution at the time of scission are reflected in the width of the energy distribution, the constancy of the measured width suggests rather similar scission configurations and thermal distributions,

independent of the atomic number of the ternary fragment (for Z≥4). For reference we have also shown as open symbols the measured[10] second moment of the ^{4}He, Li, and Be energy distributions in spontaneous fission of ^{252}Cf (*cold* fission). The differences in the widths for *hot* and *cold* fission may also indicate a broader distribution in scission configurations leading to *hot* ternary fission.

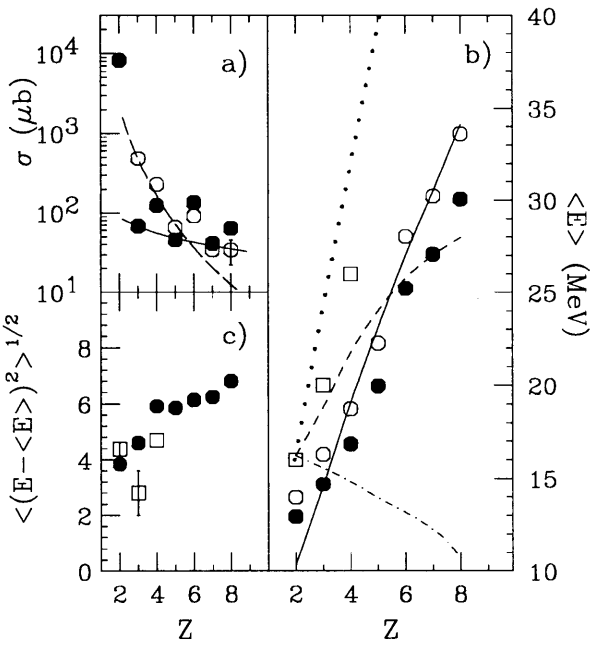

Figure 3. Panel a): Dependence of the emitted IMF cross-section on the atomic number of the neck fragment; closed circles: neck fragments; open circles: isotropic fragments. Panels b-c): Dependence of the first and second moments of the low energy and high energy components of the energy spectra on the atomic number of the neck fragment. Solid symbols in panel b) correspond to the measured moments. Open symbols depict the first moment transformed into the center-of-mass frame. Squares refer to ^{252}Cf fission.

In order to examine the observed trends quantitatively we have compared our observations with the predictions of a classical trajectory model.[12] In this model, the two fission fragments and the neck fragment interact as point charges. The system, consisting of the two fission fragments and the neck fragment, was assumed to be Z=90, A=232. The two fission fragments were chosen to have an initial separation distance D=26 fm, in agreement with the fission fragments having attained half of their asymptotic velocity at scission.[12] Choice of a smaller initial separation distance (e.g. D=20 fm) requires a reduction in the initial fission and IMF velocities to reproduce the asymptotic kinetic energies. The charges and masses of the two fragments were chosen based on symmetric fission. The neck fragment was specified by its charge, mass, initial position, initial kinetic energy, and the direction of its initial velocity. The initial position was chosen to be halfway between the two fission fragments (X=Y=0).[12] The IMF was emitted orthogonal to the scission axis (θ=90°).[12] For our trajectory calculations we chose initial conditions that reproduced the phenomenon of neck emission of α particles in spontaneous fission of ^{252}Cf.[12]

If the initial energy of the fragment is given by the uncertainty in its momentum due to localization of the fragment in the neck zone, it should be inversely related to the mass of the fragment.[11] Allowing the initial energy to be given by $E_{initial}$=16 MeV/$A_{fragment}$

Ref. 11 yields the dot-dashed line in Fig. 3b). The predicted Z dependence shows the opposite trend of the measured Z dependence – it decreases monotonically with increasing Z. This trend indicates that the initial kinetic energy of the neck fragment exceeds the minimum required by the uncertainty relation. If we fix the initial energy of the neck fragment at 4 MeV, the dependence of $\langle E \rangle$ on Z is in approximate agreement with the experimental data, as shown in Fig. 3b) (dashed line). We also explored fixing the initial velocity of the neck fragment (v=1.39 cm/ns). The resulting dependence of $\langle E \rangle$ on Z (dotted line) is in reasonable agreement with the ^{252}Cf data but significantly overpredicts the present experimental data, particularly for the heavier IMFs. Reasonable agreement with the present experimental data is achieved in a constant-velocity scenario if an initial velocity of 0.77 cm/ns is assumed (solid line).

‡ Present address: Department of Chemistry, Purdue University, West Lafayette, IN

† Present address: Pathologists Associated, 2401 West University Ave., Muncie, IN 47302

1. D.E. Fields *et al.,* Phys. Rev. Lett. **69**, 3713 (1992).
2. Z. Fraenkel and S.G. Thompson, Phys. Rev. Lett., **14**, 438 (1964).
3. W.W. Wilcke *et al.,* Phys. Rev. Lett. **51**, 99 (1983).
4. R. Lacey *et al.,* Phys. Rev. C **37**, 2540 (1988).
5. K. Siwek-Wilczynska *et al.,* Phys. Rev. C **48**, 228 (1993).
6. H. Ikezoe *et al.,* Phys. Rev. C **49**, 968 (1994).
7. M. Fatyga, Ph.D. thesis, Indiana University, (1987).
8. S.W. Cosper, J. Cerny, and R.C. Gatti, Phys. Rev. **154**, 1193 (1967).
9. D.E. Fields, Ph.D. thesis, Indiana University (1992).
10. S.L. Whetstone, Jr. and T.D. Thomas, Phys. Rev. **154**, 1174 (1962).
11. I. Halpern, Physics and Chemistry of Fission, International Atomic Energy Agency, Vienna, 1965, vol. 2 p. 369.
12. Y. Boneh *et al.,* Phys. Rev. **156**, 1305 (1967).

EXCLUSIVE STUDIES OF CHARGED-PARTICLE EMISSION IN ^{1}H– and ^{3}He–INDUCED REACTIONS ON HEAVY NUCLEI

D.S. Ginger, E. Cornell, W.-C. Hsi, K. Kwiatkowski, R.T. de Souza, V.E. Viola, G. Wang, and N.R. Yoder
Indiana University Cyclotron Facility, Bloomington, Indiana 47408

R.G. Korteling
Simon Fraser University, Burnaby, British Columbia, Canada V5A 1S6

Nonequilibrium and equilibrium mechanisms of complex fragment emission have been investigated in the Fermi-energy/pion-threshold regime with the ISiS 4π detector array.